

# A Reduced Extracellular Serotonin Level Increases the 5-HT<sub>1A</sub> PET Ligand <sup>18</sup>F-MPPF Binding in the Rat Hippocampus

Luc Zimmer, PharmD, PhD<sup>1,2</sup>; Latifa Rbah, MS<sup>1</sup>; Fabrice Giacomelli, MS<sup>3</sup>; Didier Le Bars, PharmD, PhD<sup>1</sup>; and Bernard Renaud, PhD<sup>2</sup>

<sup>1</sup>Centre d'Exploration et de Recherche Médicales par Émission de Positons, Biomedical Cyclotron, Lyon, France; <sup>2</sup>Institut National de la Santé et de la Recherche Médicale, Unité 512, Neurochimie et Neuropharmacologie, Lyon 1 University, Lyon, France; and <sup>3</sup>Cyclotron Research Center, Liège University, Liège, Belgium

4,2'-(Methoxyphenyl)-1-[2'-(*N*-2"-pyridinyl)-*p*-fluorobenzamido]ethylpiperazine (<sup>18</sup>F-MPPF) is a radiotracer used in clinical PET studies for the visualization of serotonin-1A (5-HT<sub>1A</sub>) receptors. In a previous study, we demonstrated that a rapid enhancement of extracellular serotonin concentrations influences <sup>18</sup>F-MPPF-specific binding. Because endogenous serotonin is significantly decreased in some pathologies, the aim of this study was to determine whether <sup>18</sup>F-MPPF is sensitive to depletion of this neurotransmitter. **Methods:** Using the β-microprobe, an original β<sup>+</sup>-sensitive intracerebral probe, and microdialysis, the effect of decreased serotonin on the specific binding of <sup>18</sup>F-MPPF to 5-HT<sub>1A</sub> receptors was investigated in the hippocampus of the anesthetized rat. Extracellular serotonin was pharmacologically decreased in the hippocampus after a single injection of *p*-ethynylphenylalanine ([*p*-EPA] 5 mg/kg), a new tryptophan hydroxylase inhibitor. **Results:** Our results showed that the <sup>18</sup>F-MPPF-specific binding was significantly enhanced after the decrease of extracellular serotonin. These results were confirmed by the <sup>18</sup>F-MPPF distribution in cerebral tissues (hippocampus-to-cerebellum ratio) and by the decrease of the extracellular <sup>18</sup>F-MPPF collected in hippocampal dialysates. **Conclusion:** This study further supports the view that <sup>18</sup>F-MPPF binding potential is increased in the hippocampus if the endogenous serotonin is pharmacologically decreased after a *p*-EPA injection. This phenomenon will be an additional factor in the interpretation of the results from <sup>18</sup>F-MPPF clinical PET studies.

**Key Words:** serotonin receptors; *p*-ethynylphenylalanine; 4,2'-(methoxyphenyl)-1-[2'-(*N*-2"-pyridinyl)-*p*-fluorobenzamido]ethylpiperazine; serotonin; microdialysis; β-microprobe

**J Nucl Med 2003; 44:1495–1501**

**T**he serotonin-1A (5-HT<sub>1A</sub>) receptor has been implicated in various affective disorders such as anxiety and depression (1–4). Thus, the functional imaging of these receptors by PET may have important implications for our understanding of the role of this receptor in those pathologies and their therapeutics.

Several radioligands have been developed for the imaging and quantification of 5-HT<sub>1A</sub> receptors using PET and have been tested in humans (5). Recently, the selective 5-HT<sub>1A</sub> antagonist, 4,2'-(methoxyphenyl)-1-[2'-(*N*-2"-pyridinyl)-*p*-fluorobenzamido]ethylpiperazine (MPPF), has successfully been labeled with <sup>18</sup>F-fluorine, resulting in the <sup>18</sup>F-fluoro analog, <sup>18</sup>F-MPPF (6). Animal experiments have shown a regional distribution of this radioligand that concurs well with known 5-HT<sub>1A</sub> receptor densities (6–10). In a recent study, we demonstrated that the <sup>18</sup>F-MPPF-specific binding was decreased after a fenfluramine-induced serotonin increase (11).

Because recent theories of the pathophysiology of depression have put much emphasis on deficiency of serotonergic function (12,13), it was of great interest to know the vulnerability of <sup>18</sup>F-MPPF to this neurotransmitter reduction but little information is currently available concerning this parameter. A recent study of 6 healthy volunteers showed that <sup>18</sup>F-MPPF binding was not affected after a dietary depletion of tryptophan, supposed to reduce the serotonin synthesis (14). However, the methodologic limit inherent in this clinical study was the lack of effective control of the brain serotonin depletion.

Therefore, this preclinical study was aimed at determining whether <sup>18</sup>F-MPPF-specific binding in the rat hippocampus is influenced after a controlled depletion of serotonin. For this purpose, we used a new tryptophan hydroxylase inhibitor, the *p*-ethynylphenylalanine (*p*-EPA), that we previously characterized (15). Accordingly, we determined in the rat hippocampus (a) the ability of *p*-EPA to decrease the extracellular serotonin, (b) the <sup>18</sup>F-MPPF tissue distribution after *p*-EPA-induced serotonin depletion, (c)

Received Jan. 13, 2003; revision accepted Apr. 21, 2003.  
For correspondence or reprints contact: Luc Zimmer, PharmD, PhD, Centre d'Exploration et de Recherche Médicales par Émission de Positons, Biomedical Cyclotron, 59 Boulevard Pinel, F-69003 Lyon, France.  
E-mail: [zimmer@cermep.fr](mailto:zimmer@cermep.fr)

the dynamic  $^{18}\text{F}$ -MPPF binding using a new intracerebral  $\beta$ -sensitive detector (the  $\beta$ -microprobe) in control rats in comparison with p-EPA-treated rats, and (d) the extracellular free  $^{18}\text{F}$ -MPPF using microdialysis during this pharmacologic challenge. Finally, we discussed several mechanisms underlying the sensitivity of  $^{18}\text{F}$ -MPPF to serotonin depletion.

## MATERIALS AND METHODS

### Drugs

Free p-EPA was synthesized as described (16), and the chemical purity of the final compound was >99%. Briefly, p-EPA was produced by the Heck reaction of trimethylsilylacetylene with *N*-*tert*-butyloxy-carbonyl-4-iodo-L-phenylalanine methyl ester followed by removal of the protecting groups. The p-EPA was dissolved in saline before animal injections.

$^{18}\text{F}$ -MPPF was synthesized with a radiochemical yield of 25% (decay corrected) in an automated synthesizer (17), using the chemical pathway previously described (8). Chemical and radiochemical purity were >98% as determined by high-performance liquid chromatography (HPLC). Specific activity from the injected radiotracer ranged from  $74 \times 10^3$  MBq/ $\mu\text{mol}$  to  $148 \times 10^3$  MBq/ $\mu\text{mol}$  (2–4 Ci/ $\mu\text{mol}$ ).

### Animal Procedures

A total of 44 male Sprague–Dawley rats (Elevage Dépré) weighing 300–400 g were used in this study. All experimental procedures were in compliance with European Economic Commission guidelines and directives (86/09/EEC). During all experiments, the rats were anesthetized by a single intraperitoneal injection of urethane (Sigma-Aldrich) at a dose of 1.7 g/kg body weight and remained anesthetized throughout all procedures. A catheter was inserted in the tail vein, allowing the injection of the radioactive tracer ( $^{18}\text{F}$ -MPPF). After all experiments, the rats were sacrificed by a KCl intravenous injection.

### $^{18}\text{F}$ -MPPF Tissue Distribution

Nine anesthetized rats were injected intraperitoneally with p-EPA (5 mg/kg) and 9 were injected with saline (control rats). Four hours after p-EPA (or saline) injection, each rat received a 37-MBq  $^{18}\text{F}$ -MPPF intravenous injection. The rats were killed by decapitation at 30, 45, and 60 min after  $^{18}\text{F}$ -MPPF injection ( $n = 3$  per time for p-EPA-treated and control rats). The brains were carefully removed and immediately dissected on an ice-cooled glass plate. The hippocampus and the cerebellum were dissected free-hand. The dissected tissues were blotted and rinsed with water to removed adhering blood and placed in preweighed counting vials. The radioactivity of each sample was measured (Cobra II auto- $\gamma$ -counter; Packard), the sample was weighed, and the activity was expressed per gram of tissue.

### Determination of Extracellular Serotonin

After urethane anesthesia, each rat was positioned on a stereotactic apparatus (LPC). The skull was exposed and the bregma point was visualized. A microdialysis probe (polycarbonate, 15-kDa cutoff, 3-mm length; CMA/Microdialysis) was implanted into the hippocampus (anteroposterior [A/P]  $-5.0$ , lateromedial [L/M]  $-5.0$ , and ventrodorsal [V/D]  $-8.0$ ) according to the atlas of Paxinos and Watson (18). The probe was immediately and continuously perfused with perfusion buffer (Dulbecco's modified

medium + 2.2 mmol/L  $\text{CaCl}_2$ ) at 1.0  $\mu\text{L}/\text{min}$  using a microsyringe pump. Body temperature was maintained at  $37^\circ\text{C} \pm 1^\circ\text{C}$  throughout the test period using a thermostatically controlled heating blanket (CMA/Microdialysis). After a 2-h equilibrium period, 10-min dialysate samples were collected and were defined as basal level before drug (p-EPA, 5 mg/kg intraperitoneally) or saline injection (control rats). The serotonin content in dialysates was assayed using HPLC with an electrochemical detector (Antec Leyden). We used a  $\text{C}_{18}$  reverse-phase column (Uptisphere ODB, 3  $\mu\text{m}$ ,  $100 \times 2$  mm; Interchim); the mobile phase, delivered at a rate of 0.3 mL/min, was composed of 75 mmol/L  $\text{NaH}_2\text{PO}_4$ , 0.1 mmol/L ethylenediaminetetraacetic acid, 0.3 mmol/L octanesulfonic acid, and 18% methanol (pH 4.3). In these conditions, the retention time for serotonin was 5.0 min, and its detection limit was 0.5 pg per sample (10  $\mu\text{L}$ ).

### Determination of $^{18}\text{F}$ -MPPF Binding

The  $\beta$ -microprobe apparatus, previously named "SIC" (19), is the prototype of a  $\beta$ -sensitive microprobe stereotactically implanted in the rat brain, designed and manufactured by the Institut of Physique Nucléaire (Orsay, France). The sensitive end of the probe consists of a 1-mm-length and 1-mm-diameter plastic scintillating fiber, allowing definition of the detection volume surrounding the probe. The detection tip is coupled to a single-photon counting photomultiplier (R7400P; Hamamatsu). An interface module ensures the readout of the photomultiplier signal through an amplifier integrator and the radiotracer kinetics are visualized in real time.

After rat anesthesia and catheterization of the tail vein, 1  $\beta$ -microprobe was implanted in the hippocampus, and the second was implanted in the cerebellum. The coordinates of implantation were as follows: A/P  $-5.0$ , L/M 5.0, and V/D  $-8.0$  (hippocampus); A/P  $-12.0$ , L/M 3.0, and V/D  $-4.0$  (cerebellum), from the bregma point and the dura, respectively. Body temperature was maintained at  $37^\circ\text{C} \pm 1^\circ\text{C}$  throughout the test period using a thermostatically controlled heating blanket (CMA/Microdialysis).

$\beta$ -Microprobe acquisition was performed 2 h after implantation of the probes according to our previous studies (11,19). This time period corresponds with the neurotransmission stabilization period (20). For each acquisition, 37 MBq  $^{18}\text{F}$ -MPPF (in a volume of 0.4 mL saline) were injected via the tail vein over a 45-s period. This activity corresponded to a stable content of 250–500 pmol. The time course of radioactivity was studied for 90 min using 10-s time integration acquisition.

In a first group of rats, each anesthetized rat received a p-EPA injection (5 mg/kg intraperitoneally in 0.3 mL of saline) followed at 4 h by a 37-MBq  $^{18}\text{F}$ -MPPF injection. The  $^{18}\text{F}$ -MPPF binding was measured with the  $\beta$ -microprobe in the hippocampus and the cerebellum. In a second group (control rats), each anesthetized rat received a saline injection followed at 4 h by a 37-MBq  $^{18}\text{F}$ -MPPF injection. After completion of experiments, animals were sacrificed and probe placements were verified using the atlas of Paxinos and Watson (18).

### Determination of Extracellular $^{18}\text{F}$ -MPPF

Eight anesthetized rats were implanted with 2 microdialysis probes (1 in the hippocampus and 1 in the cerebellum, according to the above coordinates). Four rats were injected intraperitoneally with p-EPA (5 mg/kg) and 4 rats were injected with saline (control rats). The probes were continuously perfused with perfusion buffer at 1.0  $\mu\text{L}/\text{min}$ . Body temperature was maintained at  $37^\circ\text{C} \pm 1^\circ\text{C}$  throughout the test period using a thermostatically controlled heat-

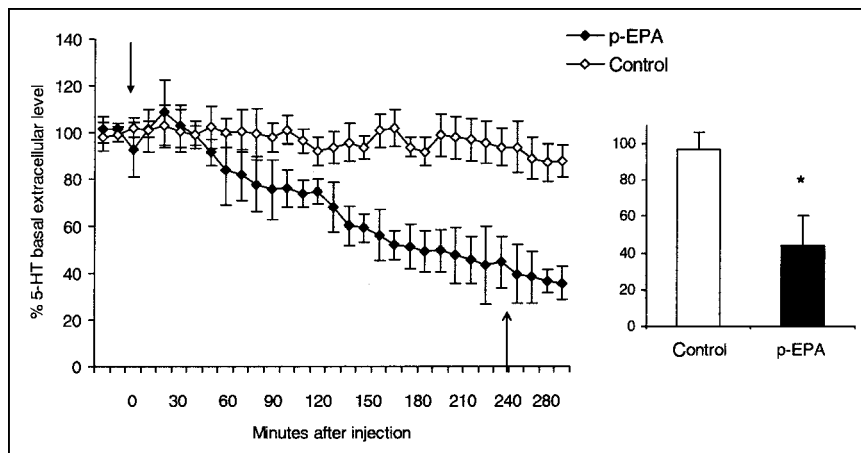


**FIGURE 1.** Effect of single p-EPA injection (5 mg/kg intraperitoneally) on dialysate level of serotonin in hippocampus of anesthetized rats. Same number of rats ( $n = 4$ ) was used for both p-EPA injection and saline injection (control rats). Data are mean values  $\pm$  SEM expressed as percentage of basal levels. Arrow ( $\downarrow$ ) denotes p-EPA injection. Arrow ( $\uparrow$ ) denotes  $^{18}\text{F}$ -MPPF injection, 4 h after p-EPA injection, when serotonin (5-HT) level is 60% lower in p-EPA-treated rats than in control rats (inset,  $*P < 0.05$ ).

ing blanket. Four hours after p-EPA (or saline) injection, each rat received a 37-MBq  $^{18}\text{F}$ -MPPF intravenous injection. Dialysates were collected every 5 min (5  $\mu\text{L}$ ) in both areas, and the radioactivity of the dialysates was measured using an automated  $\gamma$ -counter (Cobra II, Packard) calibrated in the  $^{18}\text{F}$  energy range. After completion of experiments, animals were sacrificed and probe placements were verified using the atlas of Paxinos and Watson (18).

#### Data Analysis

The  $\beta$ -microprobe data (expressed as mean of disintegration per 10 s) were averaged every minute. These data were corrected for radioactive decay and normalized with respect to the activity injected. Statistical analysis was conducted by comparing the mean values obtained from both the control and the treated animals for each time point (every min) using 1-way ANOVA on repeated measurements, followed by a post hoc Student  $t$  test.  $P < 0.05$  was considered to be statistically significant.

## RESULTS

### Effect of p-EPA on Extracellular Serotonin

The electrochemical measurement of serotonin in dialysates showed that during the control experiment, the level of the neurotransmitter in the hippocampus did not significantly change ( $1.6 \pm 0.1$  fmol/ $\mu\text{L}$  without probe correction). The p-EPA injection induced a significant and gradual decrease in extracellular serotonin in the hippocampus (Fig. 1). Four hours after the p-EPA injection, the extracellular serotonin level was significantly lower, amounting to a 60% reduction in comparison with the control rats (Fig. 1, inset).

### $^{18}\text{F}$ -MPPF Tissue Distribution

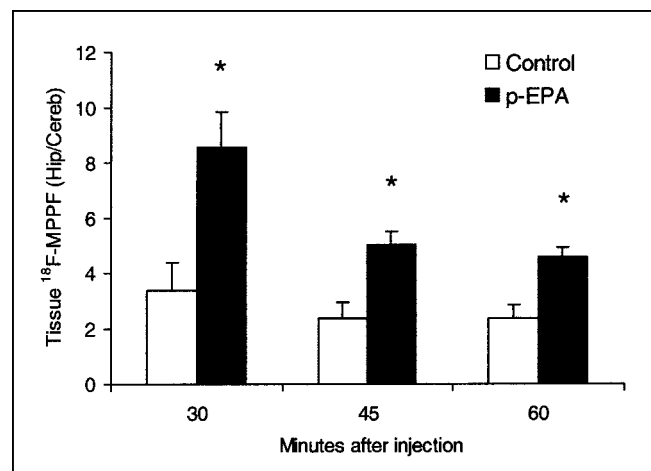
In the dissected tissues of control rats ( $n = 3$  rats at each time), the hippocampal  $^{18}\text{F}$ -MPPF concentrations were 3.5-, 2.5-, and 2.4-fold higher than those found in the cerebellum at 30, 45, and 60 min, respectively (Fig. 2). In p-EPA-injected rats ( $n = 3$  rats at each time), the hippocampal  $^{18}\text{F}$ -MPPF concentrations were 8.5-, 5-, and 4.6-fold higher than those determined in the cerebellum at 30, 45, and 60 min, respectively. Our results showed that, in the hippocampus of p-EPA-treated rats, the  $^{18}\text{F}$ -MPPF concentrations were significantly increased in comparison with the control

rats injected with saline ( $P < 0.05$ ), whereas the  $^{18}\text{F}$ -MPPF concentrations in the cerebellum remained unchanged between the p-EPA-treated and the control rats.

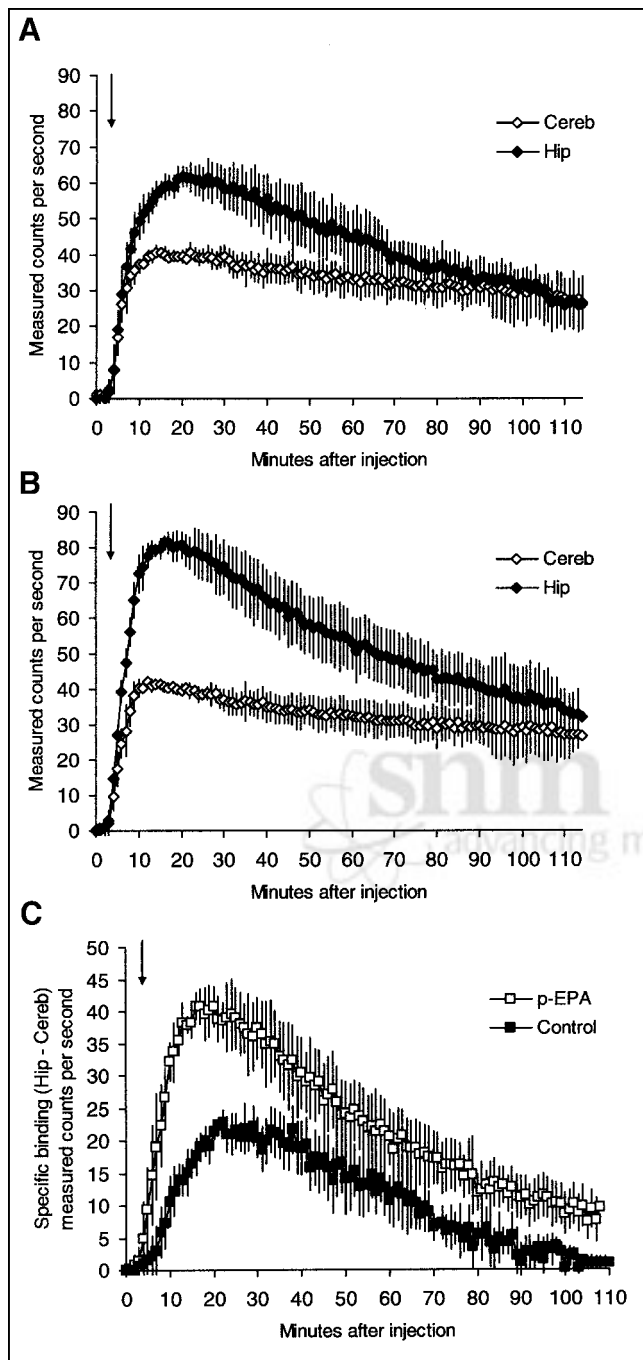
### Radioactivity Kinetic Curves of $^{18}\text{F}$ -MPPF

Figure 3A shows the radioactivity kinetic curves of  $^{18}\text{F}$ -MPPF in the hippocampus and the cerebellum of control rats. A maximal amount of radioactivity had already accumulated in the hippocampus 20 min after administration of  $^{18}\text{F}$ -MPPF, resulting in a hippocampus-to-cerebellum ratio  $\approx 1.55$  ( $n = 5$  rats). Twenty minutes after injection, the hippocampal radioactivity decreased slowly and became similar to cerebellar radioactivity by 70 min after injection.

Figure 3B shows the radioactivity kinetic curves of  $^{18}\text{F}$ -MPPF in the hippocampus and the cerebellum of p-EPA-treated rats. The maximal amount of radioactivity had already accumulated in the hippocampus 17 min after administration of  $^{18}\text{F}$ -MPPF, resulting in a hippocampus-to-



**FIGURE 2.** Hippocampus (Hip) vs. cerebellum (Cereb) ratios of total tissue radioactivity from 30 to 60 min after intravenous injection of  $^{18}\text{F}$ -MPPF. Experiments were performed in control rats ( $n = 9$ ) and in rats that were injected with p-EPA 4 h earlier ( $n = 9$ ). Data are mean values  $\pm$  SEM (3 rats per time group). \*Significant increase of ratio was obtained for p-EPA-treated rats ( $P < 0.05$ ).



**FIGURE 3.** (A) Radioactivity kinetic curve measured by  $\beta$ -microprobe in hippocampus (Hip) and cerebellum (Cereb) of control rats after 37-MBq  $^{18}\text{F}$ -MPPF injection (10-s acquisition averaged every min; mean of 5 rats  $\pm$  SEM). Arrow ( $\downarrow$ ) indicates  $^{18}\text{F}$ -MPPF injection. (B)  $^{18}\text{F}$ -MPPF radioactivity kinetic curve measured by  $\beta$ -microprobe in hippocampus and cerebellum of p-EPA-treated rats (mean of 5 rats  $\pm$  SEM). Arrow ( $\downarrow$ ) indicates  $^{18}\text{F}$ -MPPF injection. (C) Specific binding of  $^{18}\text{F}$ -MPPF calculated by cerebellar activity deducted from hippocampus activity ( $n = 5$  rats for each group  $\pm$  SEM). Arrow ( $\downarrow$ ) indicates  $^{18}\text{F}$ -MPPF injection. Values of p-EPA-treated rat curve are significantly higher than those of control rat curve ( $P < 0.05$ ).

cerebellum ratio  $\approx 2$  ( $n = 5$  rats). Twenty minutes after injection, hippocampal radioactivity decreased slowly and became similar to cerebellar radioactivity by 90 min after injection.

In control rats, the  $^{18}\text{F}$ -MPPF-specific binding, calculated by subtracting cerebellar activity from hippocampal activity, averaged 20 counts/second (cps) 30 min after injection and became nil 90 min after  $^{18}\text{F}$ -MPPF injection (Fig. 3C). In p-EPA-treated rats, the  $^{18}\text{F}$ -MPPF-specific binding averaged 40 cps 20 min after injection and was significantly increased in comparison with the control rats ( $P < 0.05$ ). These specific binding values were significantly higher than those in control rats during all  $\beta$ -microprobe acquisition ( $P < 0.05$ ) and reached 10 cps 90 min after the  $^{18}\text{F}$ -MPPF injection. It should be noted that the level of radioactivity in the cerebellum was not affected by p-EPA treatment.

#### Extracellular $^{18}\text{F}$ -MPPF

Figure 4 represents the variation of the extracellular radioactivity of  $^{18}\text{F}$ -MPPF in the hippocampus (Fig. 4A) and the cerebellum (Fig. 4B) in rats having undergone implantation of 2 microdialysis probes: 1 in the cerebellum and 1 in the hippocampus. In p-EPA-treated rats, significantly

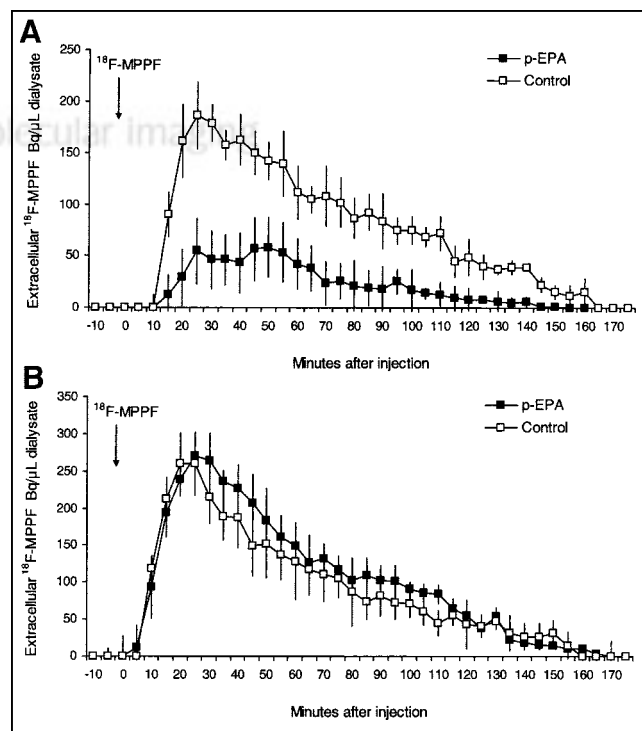


**FIGURE 4.** (A) Extracellular radioactivity, measured by auto- $\gamma$ -counter, of dialysates collected every 5 min from hippocampus of anesthetized rats after 37-MBq  $^{18}\text{F}$ -MPPF intravenous injection into p-EPA-treated rats ( $n = 4$  rats  $\pm$  SEM) and control rats ( $n = 4$  rats  $\pm$  SEM). Arrow ( $\downarrow$ ) indicates  $^{18}\text{F}$ -MPPF injection. (B) Extracellular radioactivity, measured by auto- $\gamma$ -counter, of dialysates collected every 5 min from cerebellum of same rats as in A after 37-MBq  $^{18}\text{F}$ -MPPF intravenous injection into p-EPA-treated rats ( $n = 4$  rats  $\pm$  SEM) and control rats ( $n = 4$  rats  $\pm$  SEM). Arrow ( $\downarrow$ ) indicates  $^{18}\text{F}$ -MPPF injection.

less extracellular  $^{18}\text{F}$ -MPPF was collected in the hippocampal dialysates in comparison with the control rats ( $P < 0.05$ ;  $n = 4$  for each group). At the same time, the extracellular radioactivity in the cerebellum was unchanged after p-EPA injection in comparison with control rats.

## DISCUSSION

$^{18}\text{F}$ -MPPF demonstrates cerebral binding that is consistent with the distribution of 5-HT<sub>1A</sub> receptors, evidenced by a high uptake in the hippocampus and no uptake in the receptor-poor cerebellum (7,11). This property enables its use in clinical PET studies for the visualization of 5-HT<sub>1A</sub> receptors (21–23) and their quantification (24).

We demonstrated recently that  $^{18}\text{F}$ -MPPF binding in the rat hippocampus is directly influenced by the increase of the extracellular serotonin after fenfluramine injection (11). However, for an optimal use of  $^{18}\text{F}$ -MPPF in clinical studies, it is important to investigate whether the binding of the radiotracer is sensitive to partial serotonin depletion. Particularly, it is hypothesized that psychiatric disorders such as depression are probably associated with a serotonin decrease (12,13). Therefore, our aim was to study the vulnerability of  $^{18}\text{F}$ -MPPF to a provoked decrease of extracellular serotonin.

To achieve a controlled depletion in serotonin, we used a new molecule, called p-EPA, which is a specific inhibitor of tryptophan hydroxylase (25). In a recent study, we demonstrated that p-EPA is a useful pharmacologic tool, which powerfully and rapidly reduces the level of extracellular serotonin (15). Our current microdialysis results confirmed that, at a short time after p-EPA administration, extracellular serotonin was depleted to a significant extent in the hippocampus (–60%, 4 h after injection). This 4-h delay after p-EPA injection was chosen to allow a partial serotonin depletion that may be of greater theoretic interest with respect to both the physiologic regulation of serotonin function and its implication in depression, for example (26,27).

In the first experiments exploring the tissue distribution of radioactivity, the increased accumulation of  $^{18}\text{F}$ -MPPF in the hippocampus after p-EPA injection highlighted the sensitivity of  $^{18}\text{F}$ -MPPF to serotonin decrease. Therefore, it was of great interest to monitor  $^{18}\text{F}$ -MPPF binding kinetics using the  $\beta$ -microprobe device previously validated (11,19,28). In addition to the hippocampal  $\beta$ -microprobe, we implanted another  $\beta$ -microprobe in the cerebellum. The specific binding was estimated as the difference between the concentration of radioligand in the region of interest—the hippocampus—and the region of reference—the cerebellum, which is practically devoid of 5-HT<sub>1A</sub> receptors (21,22). After intravenous administration into control rats, the  $^{18}\text{F}$ -MPPF time-radioactivity curves obtained with the  $\beta$ -microprobe were reproducible between rats (coefficient of variation  $\approx 10\%$ ), showing a clear separation between the hippocampus and the cerebellum. In control rats, the hippocampal curve became similar to the cerebellar curve 70 min after  $^{18}\text{F}$ -MPPF

injection. In p-EPA-treated rats, the  $\beta$ -microprobe measurements revealed that the magnitude of the  $^{18}\text{F}$ -MPPF-specific binding was significantly increased. The difference between the hippocampus-to-cerebellum ratio obtained with the  $\beta$ -microprobe ( $\sim 2$ ) and the same ratio measured by tissue counting ( $\sim 4$ ) could be attributed to the fact that tissue values reflect mainly the tracer concentration, whereas the  $\beta$ -microprobe signal most likely integrates the tracer concentration (bound and free) and the blood radioactivity (28). It is known that blood radioactivity, 30 min after  $^{18}\text{F}$ -MPPF injection, remains high in comparison with radioactivity levels in tissue (9). Moreover, the venous sinuses are near the cerebellum when the hippocampus has only a 4%–5% blood volume (29). This probably leads to an overestimation of the cerebellar radioactivity by the  $\beta$ -microprobe.

In complementary experiments, after  $^{18}\text{F}$ -MPPF injection, the measurement of the radioactivity collected by the microdialysis probes revealed a lower extracellular radioactivity in the hippocampus of p-EPA-treated rats in comparison with control rats, whereas the cerebellar radioactivity was identical in both rat groups. The collected radioactivity in dialysates can be attributed to the  $^{18}\text{F}$ -MPPF itself because  $>90\%$  of the radioactivity in the hippocampus and the cerebellum is due to the unmetabolized compound (9). This result could be interpreted as a lower quantity of free  $^{18}\text{F}$ -MPPF in the extracellular space of the hippocampus of depleted rats, resulting from a higher fraction of  $^{18}\text{F}$ -MPPF bound to 5-HT<sub>1A</sub> receptors. In other words, after p-EPA serotonin depletion, fewer serotonin molecules occupy the 5-HT<sub>1A</sub> receptors, which, in turn, become more accessible to  $^{18}\text{F}$ -MPPF molecules. According to these results, in the hippocampus of p-EPA-treated rats, the injected  $^{18}\text{F}$ -MPPF was bound more to 5-HT<sub>1A</sub> receptors, resulting in a higher radioactivity level measured by the  $\beta$ -microprobe.

To our knowledge, this study constitutes the first demonstration that the binding of  $^{18}\text{F}$ -MPPF in the hippocampus is increased by a reduction in extracellular serotonin. Few experimental data exist that document the displacement of a PET radioligand after serotonin depletion. In recent studies of the widely used 5-HT<sub>1A</sub> radiotracer, WAY 100635, this radioligand's specific binding was unchanged after a depletion of serotonin tissue levels produced by treatment with *p*-chlorophenylalanine (30) or with reserpine (31). We explain this discrepancy in sensitivity to serotonin depletion between radiolabeled WAY 100635 and MPPF by differences in the characteristics of both radioligands. Two main factors could be evoked: the affinity of the radioligand for the 5-HT<sub>1A</sub> receptors and the lipophilicity of the radiotracer.

Seeman et al. (32) proposed initially that low-affinity radiotracers bind more “loosely” to receptors, and, therefore, are more vulnerable to neurotransmitter modifications. This classic occupancy model is regularly evoked to explain the vulnerability of PET radiotracers to endogenous competition. Because  $^{18}\text{F}$ -MPPF affinity is similar to serotonin affinity for 5-HT<sub>1A</sub> receptors—the inhibitory constant ( $K_i$ ) = 3.3 nmol/L versus 4.17 nmol/L (33,34)—the classic

occupancy model could explain, intuitively, the increase of  $^{18}\text{F}$ -MPPF binding after depletion of serotonin in the vicinity of  $5\text{-HT}_{1A}$  receptors. The comparison between  $^{18}\text{F}$ -MPPF and  $^{11}\text{C}$ -WAY 100635 provides arguments for this theory. The limited sensitivity of radiolabeled WAY 100635 to endogenous serotonin (35–37), particularly after serotonin depletion (30–31), could be explained by its higher affinity for the  $5\text{-HT}_{1A}$  receptors (33). However, we agree with Laruelle (38) that the simple binding competition theory, which implies the relative affinity of the radiotracer, is probably limited.

Another factor that might contribute to these neurotransmitter–radiotracer interactions might be the lipophilicity of  $^{18}\text{F}$ -MPPF. Over the years, several observations suggest that receptor trafficking differentially affects radioligand binding (38). This model is based on the fact that receptors are distributed between a pool of receptors externalized on the plasma membrane and a pool of receptors internalized in the endosomal compartment. The density of membrane-bound  $5\text{-HT}_{1A}$  receptors could rise when extracellular serotonin levels become lower. Thus, it cannot be excluded that, during our pharmacologic serotonin depletion, the  $5\text{-HT}_{1A}$  receptors are translocated from the intracellular to the membrane compartment. This process would result in increased availability for  $^{18}\text{F}$ -MPPF. This phenomenon implies that  $^{18}\text{F}$ -MPPF binds preferentially to the externalized receptors because its relatively low lipophilicity ( $\log P = 3.12$ , according to analysis online at <http://www.logp.com/>) could reduce its diffusion within the cell at tracer doses. On the other hand, the higher lipophilicity of  $^{11}\text{C}$ -WAY 100635 ( $\log P = 4.37$ ) should enable this ligand to diffuse within the cell and to bind equally to externalized and internalized  $5\text{-HT}_{1A}$  receptors, preventing it from detection of serotonin manipulations.

However, factors other than lipophilicity might be involved in determining the accessibility of radioligand to the internalized receptors (38). Because the receptor trafficking implies endocytosis via clathrin-coated vesicles, the acidification of the receptor environment is also likely to differentially affect  $^{18}\text{F}$ -MPPF and  $^{11}\text{C}$ -WAY 100635 binding to the intracellular  $5\text{-HT}_{1A}$  receptors. Substantive preclinical work is needed to confirm the potential importance of the occupancy model versus the internalization model for the phenomena described in this study. Particularly, it would be of great interest to model the plasma membrane's diffusion of both  $^{18}\text{F}$ -MPPF and  $^{11}\text{C}$ -WAY 100635 and their binding after the modification of the  $5\text{-HT}_{1A}$  receptor protonization.

## CONCLUSION

The main conclusion of this study is that  $^{18}\text{F}$ -MPPF-specific binding is significantly increased after a decrease in extracellular serotonin. This work provides valuable new data that complete our previous study showing the  $^{18}\text{F}$ -MPPF vulnerability to serotonin increase (11). Currently,  $^{18}\text{F}$ -MPPF is the unique in vivo  $5\text{-HT}_{1A}$  radiotracer that

could reflect modulation of serotonin levels. This radiotracer may prove useful in many studies in which it may be possible to monitor decreases and increases in serotonin levels occurring as a result of psychiatric diseases (i.e., depression) or drug treatments, respectively. Conversely, in studies in which the intention is only to quantify the  $5\text{-HT}_{1A}$  receptor density, binding competition between  $^{18}\text{F}$ -MPPF and serotonin can be an additional factor in interpreting the results of PET studies.

## REFERENCES

1. Glennon RA. Serotonin receptors: clinical implications. *Neurosci Biobehav Rev*. 1990;14:35–47.
2. Kostowski W, Plaznik A, Archer T. Possible implication of  $5\text{-HT}_{1A}$  function for the etiology and treatment of depression. *New Trends Exp Clin Psychiatry*. 1989;5:91–116.
3. Peroutka SJ.  $5\text{-HT}$  receptors: past, present and future. *Trends Neurosci*. 1995;18:68–69.
4. Saxena PR. Serotonin receptors: subtypes, functional responses and therapeutic relevance. *Pharmacol Ther*. 1995;66:339–368.
5. Pike V, Halldin C, Wikström H. Radioligands for the study of brain  $5\text{-HT}_{1A}$  receptors *in vivo*. In: King FD, Oxford AW, eds. *Progress in Medicinal Chemistry*. Amsterdam, The Netherlands: Elsevier Science; 2001:189–247.
6. Shiu CY, Shiu GG, Mozley PD, et al.  $^{18}\text{F}$ -MPPF: a potential radioligand for PET studies of  $5\text{-HT}_{1A}$  receptors in humans. *Synapse*. 1997;25:147–154.
7. Ginovart N, Hassoun W, Le Bars D, Weissmann D, Leviel V. *In vivo* characterization of  $^{18}\text{F}$ -MPPF, a fluoro analog of WAY-100635 for visualization of  $5\text{-HT}_{1A}$  receptors. *Synapse*. 2000;35:192–200.
8. Le Bars D, Lemaire C, Ginovart N, et al. High-yield radiosynthesis and preliminary *in vivo* evaluation of  $^{18}\text{F}$ -MPPF, a fluoro analog of WAY-100635. *Nucl Med Biol*. 1998;25:343–350.
9. Plenevaux A, Weissmann D, Aerts J, et al. Tissue distribution, autoradiography, and metabolism of 4-(2'-methoxyphenyl)-1-[2'-[N-(2"-pyridinyl)-p- $^{18}\text{F}$ -fluorobenzamido]ethyl]piperazine  $^{18}\text{F}$ -MPPF, a new serotonin  $5\text{-HT}_{1A}$  antagonist for positron emission tomography: an *in vivo* study in rats. *J Neurochem*. 2000;75:803–811.
10. Plenevaux A, Lemaire C, Aerts J, et al. [ $^{18}\text{F}$ ]p-MPPF: a radiolabelled antagonist for the study of  $5\text{-HT}_{1A}$  receptors with PET. *Nucl Med Biol*. 2000;27:467–471.
11. Zimmer L, Mauger G, Le Bars D, Bonmarchand G, Luxen A, Pujol JF. Effect of endogenous serotonin on the binding of the  $5\text{-HT}_{1A}$  PET ligand  $^{18}\text{F}$ -MPPF in the rat hippocampus: kinetic beta measurements combined with microdialysis. *J Neurochem*. 2002;80:278–286.
12. Curzon G. Serotonergic mechanisms of depression. *Clin Neuropharmacol*. 1988;11(suppl 2):S11–S20.
13. Stockmeier CA, Shapiro LA, Dilley GE, Kolli TN, Friedman L, Rajkowska G. Increase in serotonin-1A autoreceptors in the midbrain of suicide victims with major depression: postmortem evidence for decreased serotonin activity. *J Neurosci*. 1998;18:7394–7401.
14. Udo de Haes JI, Bosker FJ, Van Waarde A, et al.  $5\text{-HT}_{1A}$  receptor imaging in the human brain: effect of tryptophan depletion and infusion on [ $^{18}\text{F}$ ]MPPF binding. *Synapse*. 2002;46:108–115.
15. Zimmer L, Luxen A, Giacomelli F, Pujol JF. Short and long-term effects of p-ethynylphenylalanine on brain serotonin levels. *Neurochem Res*. 2002;27:269–275.
16. Kayser B, Altman J, Beck W. Alkyne bridged alpha-amino acids by palladium mediated coupling of alkynes with N-t-Boc-4-iodophenylalanine methyl ester. *Tetrahedron*. 1997;53:2475–2484.
17. Le Bars D, Bonmarchand G, Alvarez JM, Lemaire C, Mosdzianowski C. New automation of  $^{18}\text{F}$ -MPPF using a coincidence synthesizer [abstract]. *J Labelled Compds Radiopharm*. 2001;44(suppl):S1045.
18. Paxinos G, Watson C. *The Rat Brain in Stereotaxic Coordinates*. New York, NY: Academic Press; 1986:24–38.
19. Zimmer L, Hassoun W, Pain F, et al. SIC, an intracerebral  $\beta$ -range-sensitive probe for radiopharmacology investigations in small laboratory animals: binding studies with  $^{11}\text{C}$ -raclopride. *J Nucl Med*. 2002;43:227–233.
20. Benveniste H. Brain microdialysis. *J Neurochem*. 1989;52:1667–1679.
21. Passchier J, van Waarde A, Pieterman RM, et al. *In vivo* delineation of  $5\text{-HT}_{1A}$  receptors in human brain with  $^{18}\text{F}$ -MPPF. *J Nucl Med*. 2000;41:1830–1835.
22. Passchier J, van Waarde A, Pieterman RM, et al. Quantitative imaging of  $5\text{-HT}_{1A}$

- receptor binding in healthy volunteers with  $^{18}\text{F}$ -p-MPPF. *Nucl Med Biol.* 2000;27:473–476.
23. Passchier J, van Waarde A, Vaalburg W, Willemsen AT. On the quantification of [ $^{18}\text{F}$ ]MPPF binding to 5-HT<sub>1A</sub> receptors in the human brain. *J Nucl Med.* 2001;42:1025–1031.
  24. Costes N, Merlet I, Zimmer L, et al. Modeling  $^{18}\text{F}$ -MPPF positron emission tomography kinetics for the determination of 5-hydroxytryptamine(1A) receptor concentration with multiinjection. *J Cereb Blood Flow Metab.* 2002;22:753–765.
  25. Stokes AH, Xu Y, Daunais JA, et al. p-Ethynylphenylalanine: a potent inhibitor of tryptophan hydroxylase. *J Neurochem.* 2000;74:2067–2073.
  26. Datla KP, Curzon G. Effect of p-chlorophenylalanine at moderate dosage on 5-HT and 5-HIAA concentrations in brain regions of control and p-chloroamphetamine treated rats. *Neuropharmacology.* 1996;35:315–320.
  27. Harro J, Tonissaar M, Eller M, Kask A, Oreland L. Chronic variable stress and partial 5-HT denervation by parachloroamphetamine treatment in the rat: effects on behavior and monoamine neurochemistry. *Brain Res.* 2001;899:227–239.
  28. Zimmer L, Pain F, Mauger G, et al. The potential of the Beta-Microprobe, an intracerebral radiosensitive probe, to monitor the  $^{18}\text{F}$ -MPPF binding in the rat dorsal raphe nucleus. *Eur J Nucl Med.* 2002;29:1237–1247.
  29. Gunn RN, Sargent PA, Bench CJ, et al. Tracer kinetic modeling of the 5-HT<sub>1A</sub> receptor ligand [carbonyl- $^{11}\text{C}$ ]WAY-100635 for PET. *Neuroimage.* 1998;8:426–440.
  30. Rice OV, Gatley SJ, Shen J, et al. Effects of endogenous neurotransmitters on the in vivo binding of dopamine and 5-HT radiotracers in mice. *Neuropsychopharmacology.* 2001;25:679–689.
  31. Maeda J, Suhara T, Ogawa M, et al. In vivo binding properties of [carbonyl- $^{11}\text{C}$ ]WAY-100635: effect of endogenous serotonin. *Synapse.* 2001;40:122–129.
  32. Seeman P, Guan HC, Niznik HB. Endogenous dopamine lowers the dopamine D<sub>2</sub> receptor density as measured by  $^3\text{H}$ -raclopride: implications for positron emission tomography of the human brain. *Synapse.* 1989;3:96–97.
  33. Zhuang ZP, Kung MP, Kung HF. Synthesis and evaluation of 4-(2'-methoxyphenyl)-1-[2'-(N-(2"-pyridinyl)-p-iodobenzamido)ethyl]piperazine (p-MPPI): a new iodinated 5-HT<sub>1A</sub> ligand. *J Med Chem.* 1994;37:1406–1407.
  34. van Wijngaarden I, Tulp MT, Soudijn W. The concept of selectivity in 5-HT receptor research. *Eur J Pharmacol.* 1990;188:301–312.
  35. Mathis C, Simpson N, Price J, Mahmood K, Bowman K, Mintun M. Evaluation of [C-11]WAY 100635: a potent serotonin 5-HT<sub>1A</sub> receptor antagonist [abstract]. *J Nucl Med.* 1995;36(suppl):162P.
  36. Parsey RV, Hwang DR, Simpson N, et al. PET studies of competition between [ $^{11}\text{C}$ ]carbonyl-WAY 100635 and endogenous serotonin [abstract]. *J Nucl Med.* 2001;40(suppl):29P.
  37. Hume S, Hirani E, Opacka-Juffry J, et al. Effect of 5-HT on binding of  $^{11}\text{C}$ -WAY 100635 to 5-HT<sub>1A</sub> receptors in rat brain, assessed using in vivo microdialysis and PET after fenfluramine. *Synapse.* 2001;41:150–159.
  38. Laruelle M. Imaging synaptic neurotransmission with in vivo binding competition techniques: a critical review. *J Cereb Blood Flow Metab.* 2000;20:423–451.





The Journal of  
NUCLEAR MEDICINE

## **A Reduced Extracellular Serotonin Level Increases the 5-HT<sub>1A</sub> PET Ligand <sup>18</sup>F-MPPF Binding in the Rat Hippocampus**

Luc Zimmer, Latifa Rbah, Fabrice Giacomelli, Didier Le Bars and Bernard Renaud

*J Nucl Med.* 2003;44:1495-1501.

---

This article and updated information are available at:  
<http://jnm.snmjournals.org/content/44/9/1495>

---

Information about reproducing figures, tables, or other portions of this article can be found online at:  
<http://jnm.snmjournals.org/site/misc/permission.xhtml>

Information about subscriptions to JNM can be found at:  
<http://jnm.snmjournals.org/site/subscriptions/online.xhtml>

*The Journal of Nuclear Medicine* is published monthly.  
SNMMI | Society of Nuclear Medicine and Molecular Imaging  
1850 Samuel Morse Drive, Reston, VA 20190.  
(Print ISSN: 0161-5505, Online ISSN: 2159-662X)

© Copyright 2003 SNMMI; all rights reserved.

The logo for the Society of Nuclear Medicine and Molecular Imaging (SNMMI) features the letters 'S', 'N', 'M', and 'I' in a white, sans-serif font, arranged in a 2x2 grid within a red square background. To the right of the logo, the text 'SOCIETY OF NUCLEAR MEDICINE AND MOLECULAR IMAGING' is written in a smaller, black, sans-serif font, stacked in three lines.  
SOCIETY OF  
NUCLEAR MEDICINE  
AND MOLECULAR IMAGING